Critical Fluid Light Scattering

Robert W. Gammon
Institute for Physical Science and Technology
University of Maryland

Abstract

The objective is to measure the decay rates of critical density fluctuations in a simple fluid (xenon) very near its liquid-vapor critical point using laser light scattering and photon correlation spectroscopy. Such experiments have been severely limited on earth by the presence of gravity which causes large density gradients in the sample when the compressibility diverges approaching the critical point. The goal is to measure fluctuation decay rates at least two decades closer to the critical point than is possible on earth, with a resolution of 3 μK. This will require loading the sample to 0.1% of the critical density and taking data as close as 100 μK to the critical temperature (T_c = 289.72 K). The minimum mission time of 100 hours will allow a complete range of temperature points to be covered, limited by the thermal response of the sample. Other technical problems have to be addressed such as multiple scattering and the effect of wetting layers.

We have demonstrated the ability to avoid multiple scattering by using a thin sample (100 microns), and a temperature history which can avoid wetting layers, a fast optical thermostat with satisfactory microcomputer temperature control and measurement, and accurate sample loading. With the questions of experimental art solved, there remain the important engineering tasks of mounting the experiment to maintain alignment during flight and using vibration isolation to prevent Shuttle motions from distorting the sample.

The experiment entails measurement of the scattering intensity fluctuation decay rate at two angles for each temperature and simultaneously recording the scattering intensities and sample turbidity (from the transmission). The analyzed intensity and turbidity data gives the correlation length at each temperature and locates the critical temperature.

The fluctuation decay rate data set from these measurements will provide a severe test of the generalized hydrodynamics theories of transport coefficients in the critical region. When compared to equivalent data from binary liquid critical mixtures they will test the universality of critical dynamics.

1 Introduction

Near a critical point it is possible to approach a macroscopic instability continuously through equilibrium states. This instability is the source of a continuous symmetry breaking or *ordering*. The key to understanding the anomalous phenomena observed in the critical region is the thermodynamic fluctuations. Approaching the critical point the fluctuations in the order parameter become extremely large in amplitude, show long range correlations, and decay exceedingly slowly. The large amplitude and extent of the fluctuations means that they can not longer be neglected and are truly dominating the properties of the system. This dominance of the order parameter fluctuations leads to a universality of the behavior, an independence from the details of the molecular interactions, so that descriptions of the anomalies only depends on the dimensionality of the system and the number of components of the order parameter. The prediction of asymptotic static properties near critical points is now more precise than experiments.

We now know that there are many examples of critical transitions: liquid-vapor critical points, magnetic transitions such as Curie ferromagnetic points or Neel anti-ferromagnetic points, superconductivity, the helium lambda transition, binary mixture miscibility critical points, ferroelectric Curie points, etc. All these continuous transitions share in having divergent thermodynamic fluctuations. It is the study theoretically and experimentally of these fluctuations that marks this current era of critical phenomena research.

Thermodynamic fluctuations are the variations in space and time of a thermodynamic variable from its equilibrium value. The fluctuations reflect the underlying heat modes (thermally excited microscopic material modes) of the material. From condensed matter physics point of view the divergence of fluctuations is the result of the instability of a heat mode. The eigenfrequency goes to zero at the critical point and its thermal population diverges. The energy stored in this mode diverges and this is seen in the divergence of the heat capacity. In a liquid-vapor critical point the relevant modes can be described by generalized hydrodynamics. For each wavevector $\vec{q}$ there are five modes, two sound modes, two shear modes, and a thermal diffusion mode. At the liquid-vapor critical point the diffusive density fluctuation is unstable and through couplings to the other modes from the non-linearities of hydrodynamics, the other modes are affected leading to anomalies in sound propagation and shear viscosity. These modes can be used as a basis for describing the static and dynamic properties of a material and are the fundamental excitations of the material.

Experimentally it is often possible to look directly at the microscopic excitations. Most commonly this is done with a scattering measurement where one can measure either the static or dynamic structure factors of the modes. Such measurements probe modes having wavevector magnitude q, with

$$q = 2k\sin(\theta/2) \quad ,$$

where k is the wavevector magnitude of the incident radiation and θ is the scattering angle. Measurements of the intensity versus angle gives the correlation length ξ of the fluctuations and spectroscopy of the scattered light gives the spectrum or time correlation of the modes. For liquid-vapor transitions light scattering has furnished the best method. The techniques are now highly developed and by using photon correlation measurements of the scattered laser light intensity it is possible to have accurate measurements of the space and time correlations of the critical fluid density fluctuations.

In what follows we describe the context for the proposed experiment on critical fluid light scattering named Zeno, give the Zeno Science Requirements which will produce a significant data set during a Shuttle flight, and describe the Zeno apparatus conceptual design to meet the Science Requirements.

2 The Context for Zeno

2.1 Critical Exponents and Universality

The theory of critical phenomena is overseen by an experimental fact: thermodynamic response functions are singular at a critical point; and a conjecture: the principle of universality. The theoretical approach to critical phenomena has matured in the past decade to the point where its predictive success is rivaled only by quantum electrodynamics.

The singularity of response functions suggests that they be described simply near a critical point. Measuring the distance from the critical point by the reduced temperature $t \equiv (T - T_c)/T_c$, where T_c is the critical temperature, one expects the response function $f(t)$ to satisfy a power law $f(t) \sim t^{\varsigma}$ as $t \to 0$. The value of the critical exponent ς depends on the particular function $f(t)$. Examples for a liquid-vapor critical point are:

$$\begin{aligned} \text{specific heat,} \quad & C_v \sim t^{-\alpha}, \quad \alpha = 0.110; \\ \text{correlation length,} \quad & \xi \sim t^{-\nu}, \quad \nu = 0.630; \\ \text{isothermal compressibility,} \quad & \kappa_T \sim t^{-\gamma}, \quad \gamma = 1.241. \end{aligned}$$

The universality principle makes critical exponents more than just a mathematical curiosity. Separate all critical points into universality classes, where each universality class has two unique properties: the spatial dimension of the system in question (3 for a fluid), and the degree of the order parameter for the critical point (1 for a liquid-gas critical point since the order parameter, the difference between liquid and gas densities $\rho_L - \rho_G$, is a scalar). Then, within a universality class, the critical exponents of all static properties should be universal, unvarying from system to system.

Critical exponents are a powerful way to characterize critical phenomena, but they provide a challenge for experiment. Since they are defined from the limiting, or asymptotic, behavior of the thermodynamic functions, the exponent of a particular function will

not be clearly revealed unless an experiment reaches the so-called asymptotic region. The challenge is that critical behavior is often not manifestly evident before reduced temperatures less than 10^{-6} are reached. Thus, experiments in critical phenomena are usually very concerned with penetrating ever closer to the critical point.

2.2 Critical Dynamics in Fluids

The critical fluctuations in a liquid-vapor system correspond to density fluctuations which decay isobarically by thermal diffusion. The mean square fluctuation in density is proportional to the isothermal compressibility and hence diverges with exponent $\gamma = 1.241$. From the thermal conduction equation it follows that the density fluctuation with wavevector $\vec{q}$ (its qth Fourier component) decays with a rate given by

$$\Gamma = Dq^2 \quad ,$$

with D the thermal diffusivity, which in the hydrodynamic limit $q \rightarrow 0$, is given by

$$D_0 = \frac{\Lambda}{\rho C_p} \quad ,$$

with Λ the thermal conductivity, ρ the density, and C_p the heat capacity at constant pressure. The thermal conductivity diverges approximately like ξ and C_p diverges with exponent γ. The result is that as the critical point is approached, D_0 goes to zero about like ξ^{-1}. For finite q, Γ and D approach finite limits with a strong q dependence. One of the principle results of dynamic scaling is the prediction that

$$\lim_{t \rightarrow 0} D = q^{(1+x_\eta)} \quad ,$$

where x_η is the correlation range exponent of the viscosity divergence.

2.3 The Need for Low Gravity

The techniques of temperature control in the laboratory are sufficiently advanced that it is possible to begin penetrating deeply into the critical region. However, once there it is impossible to obtain the desired result of measuring critical anomalies. The problem is gravity.

The compressibility of a fluid system diverges at the critical point: $\kappa_T \sim t^{-\gamma}$. The compressibility expresses the response of the fluid's density to pressure on the fluid. Across any fluid container, there is of course a pressure differential caused by the weight of the fluid itself: $\Delta P = \rho g h$. In normal circumstances, when a fluid is nearly incompressible, this is barely noticeable; near the critical point, the effects of the pressure differential are greatly magnified by diverging compressibility.

Under the influence of its weight, the fluid develops a density gradient; that is, fluid at the bottom of a container is more dense than fluid at the top. As the critical point is approached, the density gradient increases. What happens is that the fluid density at the extremes of the container deviates more from the critical density, and the regions of deviation grow toward each other. The net result is that only a thin layer of fluid near the center of the container is close enough to the critical density to show critical behavior; as t is reduced, the thickness of the layer decreases. This is a severe limitation for measurements on macroscopic samples.

In a light scattering experiment the laser beam used to probe the sample can only be usefully focused to a diameter of about 100 μm. When the thickness of the layer of critical fluid drops approaches this size, the light is no longer sampling a homogeneous critical system. In effect, the density gradients limit the useful range of t which can be explored. This is shown in figure 1, which gives the acceleration dependence of the limiting temperature at which the density of xenon varies by more than 1% over a 100 μm distance. At 1 g the critical point may be approached to within 14.5 mK, while at 10^{-3} g the limit is 145 μK.

This result is disappointing. At $t = 5 \times 10^{-5}$, the asymptotic region for these fluctuation wavelengths is just being reached. The decay rate for any finite wavevector will saturate at a finite, lowest value as the critical point is approached. This is shown in figure 2 for the wavevectors corresponding to the 12° and 168° scattering angles planned for Zeno. At the 1 g limit, the small angle decay rates have not yet really begun to saturate. By going to at least the 10^{-3} g limit the asymptotic behavior at both angles will be reached. This then sets the minimal requirement for reduced gravity for critical fluid light scattering. The Zeno instrument flown on the Shuttle provides a solution to this problem.

2.4 Previous Work

Progress in understanding critical phenomena has been substantial in the past decade since the methods of the renormalization group theory, first developed to solve problems in high-energy physics, have been applied to calculating the critical exponents of static divergent quantities. This theoretical work has given a computational base to the ideas of universality classes and two-scale universality, as well as accurate estimates of many critical exponents (Sengers, 1982).

In contrast, the theory of critical fluctuation dynamics and transport phenomena, although actively pursued, leaves many questions unanswered. The questions are both theoretical, because the calculations have proved difficult to perform; and experimental, because of limitations imposed by gravity as well as experimental problems with multiple scattering in light scattering experiments.

C-24

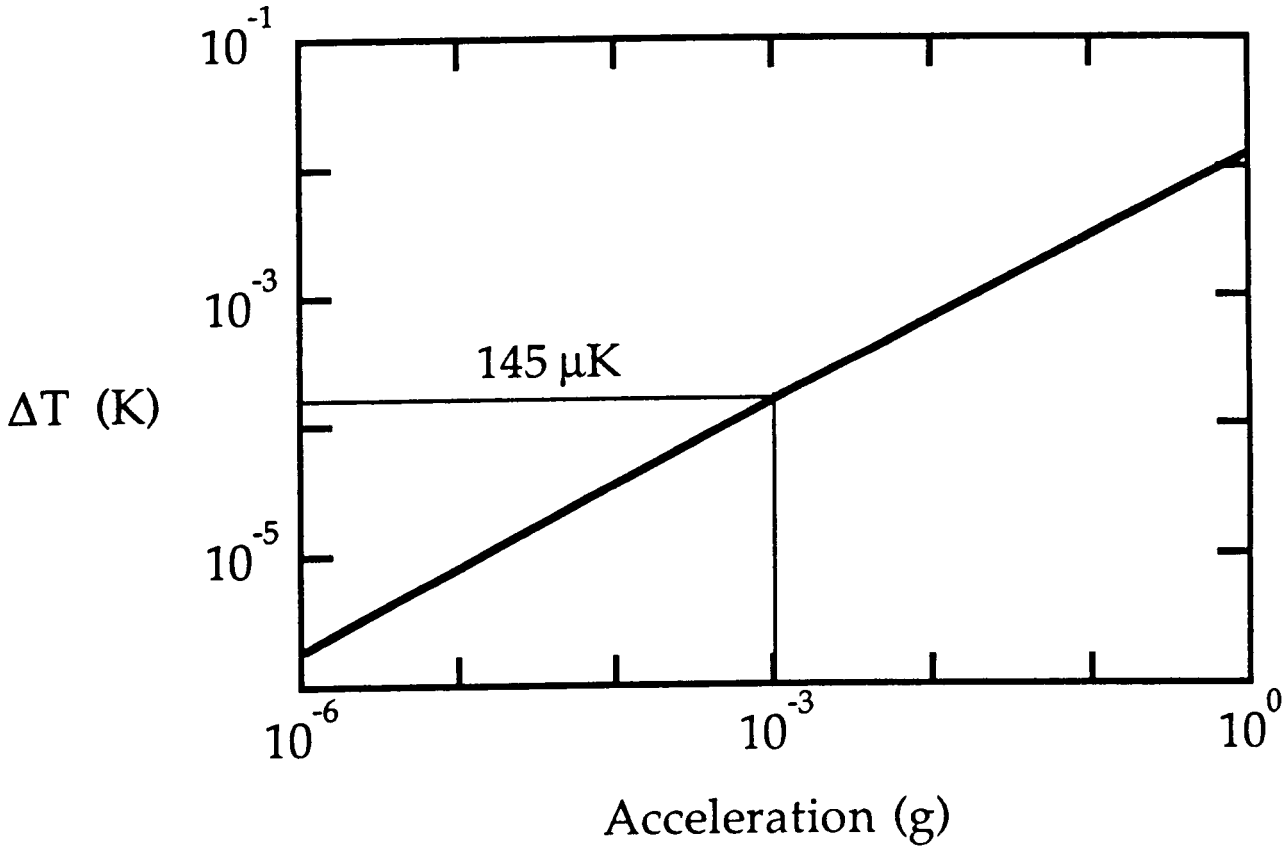

Figure 1. ΔT limit set by acceleration for 100 μm height and 1% precision.

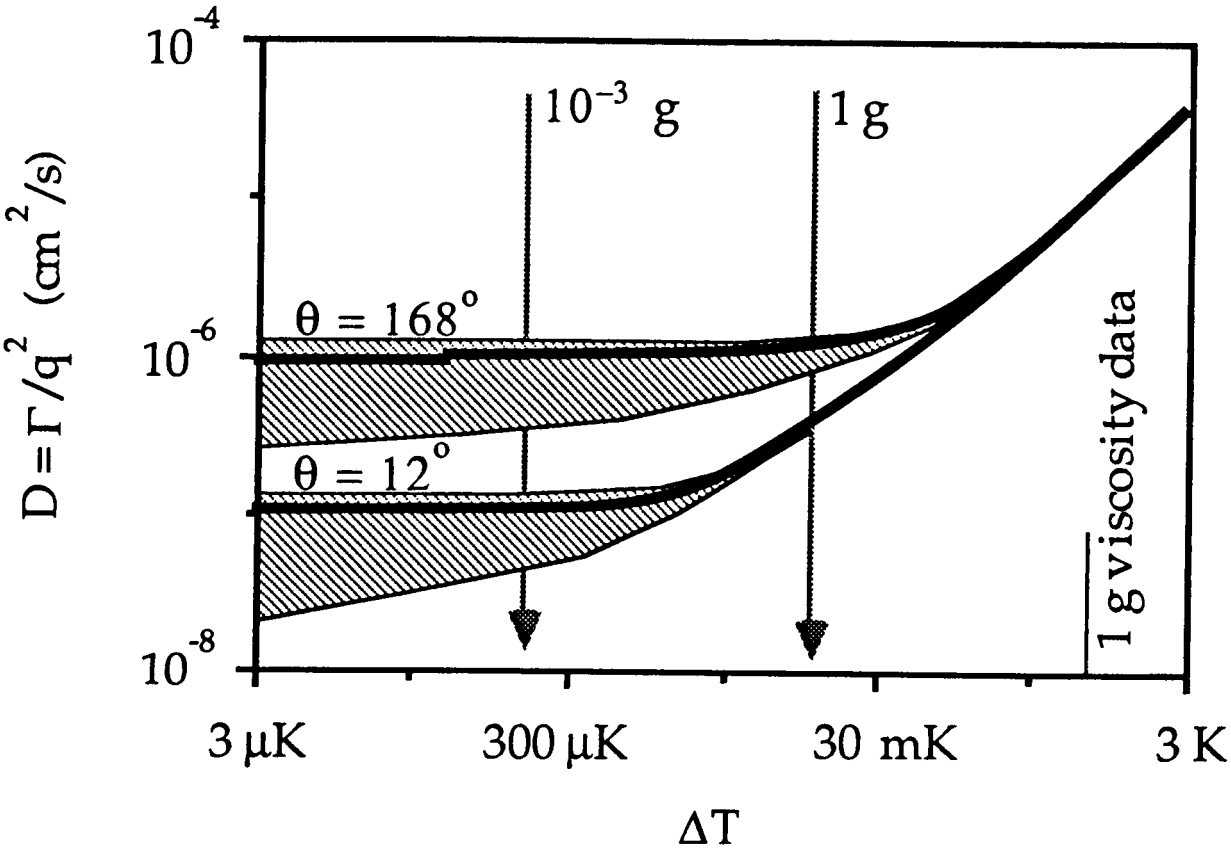

Figure 2. Calculated Xenon Diffusivity

The general state of experiment and comparison with current theory has been left at about the state of the experiments by Swinney and Henry (Swinney and Henry, 1973). Figure 3 is taken from their paper and shows the level of agreement. The quantity Γ^* is a scaled decay rate from which viscosity and angular dependence has been divided out, plotted as a function of scattering wavevectors scaled by the correlation length: $x = q\xi$. The range in x of 0.01 to 8.0 corresponds to a temperature range of 5.8 K to 3 mK from the critical temperature. The most recent and only other work on xenon was by Güttinger and Cannell (Güttinger and Cannell, 1980). They covered the same range in x with fitting errors of $\pm 5\%$ using more accurate values for ξ.

Other efforts have included work to account for multiple scattering (Bray and Chang, 1975; Reith and Swinney, 1975; Sorenson *et al.*, 1977; Beysens and Zalczer, 1977), or to avoid it altogether (Chang, Burstyn and Sengers, 1979). Particularly notable is the work by Burstyn and Sengers (1982) on the index-matched, weakly scattering binary liquid mixture 3-methylpentane-nitroethane. Excellent, precise results to 0.3 mK from its critical temperature were obtained. No significantly improved light scattering studies of the fluctuation decay rates for single component fluids have been possible.

2.5 Xenon: A Simple Fluid

Theory presumes that the liquid-gas critical point of simple fluids and the component-separation critical point of binary liquid mixtures belong to the same universality class; more specifically, that they belong to the same *static* universality class. Hence, they should exhibit the same critical behavior, at least for the static properties.

As an example of a simple fluid, xenon is without competition. The molecule is monatomic, spherically symmetric, and has no dipole moment; one expects the interatomic forces to be as simple as possible. While this would be the case for any of the noble gases, xenon wins as a choice for experimental use because it has a convenient critical temperature (16 °C), and many of its properties have been studied extensively. Nevertheless, if density-matched binary fluids, with their greater insensitivity to gravity, could apparently provide the same results on earth as a space experiment on xenon, why use xenon?

Studying critical point dynamics at a simple fluid, liquid-vapor critical point can yield better critical point measurements than in any mixture. We present the following reasons.

1. A simple fluid can be more accurately loaded to its critical density than can a mixture to its critical concentration.

2. A simple fluid reaches equilibrium more quickly after crossing the phase boundary since no time is taken for molecular diffusion to readjust the concentration profile.

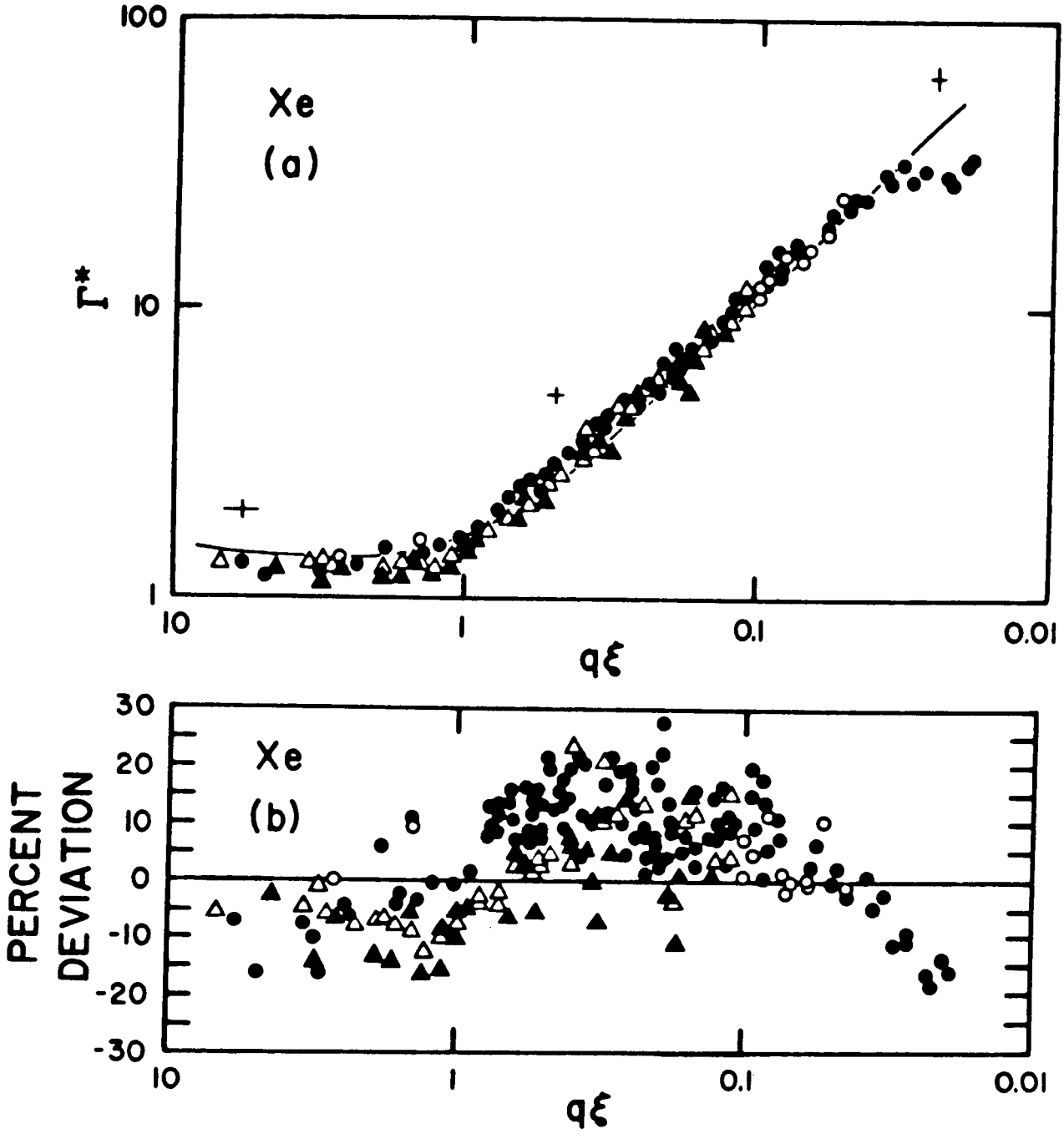

Figure 3. Reduced decay rate vs. scaled wavevector (from Swinney and Henry, 1973).

3. Simple fluid systems have smaller viscosity and correlation ranges so that the order parameter relaxation time, ξ^2 / D (D is the thermal diffusivity), is 100 times shorter than for the most favorable density-matched mixtures. This allows the measuring of viscosity one decade close to the critical temperature than for any mixture.

4. The viscosity background is smaller in the pure fluid while the amplitude of the critical part of the viscosity is about the same, making it easier to analyze the critical part.

5. A simple fluid is less susceptible to a drifting critical temperature.

6. A simple fluid has no diffusion controlled, surface wetting, sample segregation processes.

7. The order parameter in a simple fluid is identified with greater ease and certainty.

8. Additional thermodynamic measurements necessary for analyzing the dynamics into background and critical contributions exist in sufficient detail only for pure fluids.

9. Only by studying both systems can one experimentally answer the question: Do both of these fluid systems belong to the same *dynamical* universality class?

As mentioned previously, for static properties, universality classes of critical points are characterized completely by the spatial dimension of the system under study and the symmetry of its order parameter; all other properties of the system are assumed to be irrelevant. However, for dynamical properties, the static universality classes must be subdivided according to whether the order parameter is conserved in the system's dynamics. Conservation laws for other hydrodynamic variables may further subdivide universality classes (Hohenberg, 1977; Bhattacharjee and Ferrell, 1983). In contrast to pure fluids, binary liquid mixtures contain an extra hydrodynamic variable which is conserved. This is thought to be irrelevant asymptotically close to the critical temperature, although it can be relevant in the temperature range experimentally accessible on earth.

The complications that can occur when an extra degree of freedom is introduced are illustrated by the recent measurements of transport properties by Meyer and co-workers (Cohen, 1982; Cohen, 1983) near the critical point of mixtures of ^{3}He and ^{4}He. Meyer did not observe distinct composition and density fluctuations. He did observe the thermal conductivity and thermo-diffusion ratio diverging as ξ and ξ^2 respectively. To interpret Meyer's data, it was necessary to introduce the concept of the "degree of azeotropy" and to argue that the asymptotic behavior of transport properties would only become evident at reduced temperatures smaller than 10^{-5}.

Since the very careful work by Swinney and Henry and the refinement by Güttinger and Cannell on xenon, it has been clear that to apply the theories which attempt to calculate the modification of dynamic properties due to divergent fluctuations in a critical system, one needs to know the "bare" properties (without the effects of critical fluctuations) in particular of the thermal conductivity, heat capacity at constant volume, and pressure coefficient on the isochore. Then, accurate measurements of the correlation range, viscosity, and fluctuation decay rates for several wavevectors can be used to explore solutions of the coupled equations for the critical enhancements of the fluctuation lifetimes and the viscosity. Most systems do not have a large enough data base of critically evaluated properties to allow crucial comparisons. As Swinney discussed, for those systems with enough of the properties known (CO_2, SF_6, and Xe), the crucial uncertainties entering the comparison with theoretical forms are from the correlation range and the viscosity. Except for the correlation range, we still depend on the properties gathered and evaluated by Swinney and Henry in 1973.

Meanwhile, the theoretical developments of the renormalization group calculations and universality have established the static critical exponents reliably. This requires that the old data be refitted to modern forms and exponents. But, when one is finished, the fact remains that we are still extrapolating old measurements well beyond their range to provide a "test" of the new and accurate decay rate measurements. New measurements taken closer to the critical point are needed for anyone who wishes to evaluate current theoretical ideas.

2.6 Experiment and Theory at their Limit

The current theoretical treatments of dynamic critical fluctuations can be reduced to the form from generalized hydrodynamics which shows that the wavevector dependent, fluctuation corrections to the viscosity and fluctuation decay rate are coupled in a pair of integral equations over particular functions of the static structure factor (Kawasaki, 1976). Various iterative approximations to these equations have lead to several estimates for the viscosity anomaly and decay rates which differ depending on where the iteration is stopped. Bhattacharjee and Ferrell (1983) have clarified the calculation of the critical viscosity exponent, Bhattacharjee, Ferrell, Basu and Sengers (1981) showed how to treat the cross-over region of viscosity data, and Burstyn, Sengers, Bhattacharjee and Ferrell (1983) applied the calculations of the dynamic scaling function to classical fluids. Of particular interest is the prediction (Bhattacharjee and Ferrell, 1983) for the dynamic scaling exponent, i.e. the exponent, as ξ diverges, for the wavevector dependence of the decay rate, which has only been tested on binary liquid mixtures. The results for the decay rates differ from earlier estimates when the scaled wavevector becomes greater than 10. The experiment described in this document should reach scaled wavevectors of

1000.

The form suggested by Ferrell (Burstyn, 1983) for the critical part of the diffusivity is

$$D_c = \frac{\Gamma_c}{q^2} = \mathrm{R}\,\frac{kT}{6\pi\eta\xi}\,\Omega(x)\,(1+b^2x^2)^{x_\eta/2} \quad ,$$

where R is the amplitude factor, η the shear viscosity, ξ the correlation range, $x = q\xi$ the scaled wavevector, $\Omega(x) = \mathrm{K}(x)/x^2$ with $\mathrm{K}(x)$ the Kawasaki function, b the amplitude of the dynamical correction, and x_η the exponent of the correlation range in the viscosity.

The real tension between theory and experiment at present is over the viscosity exponent x_η. Siggia *et al.* (1976) suggested that $x_\eta = 0.065$ and that the amplitude, R, of the Stokes-Einstein-Kawasaki form of the decay rate was 1.20 rather than 1.00. Experiments have been rather convincing that the amplitude is 1.00, but they are not independent of the method used to estimate the correct extrapolation of the viscosity into the temperature range of the light scattering measurements. Measurements of the viscosity seem to show that the binary mixtures are best described by $x_\eta = 0.065$ (Burstyn *et al.*, 1983), but recent fitting of the available data for liquid-vapor critical systems favors the value $x_\eta = 0.054$. This is in agreement with the suggestion of Ferrell that the Siggia calculation had missed a cancellation of corrections and that the exponent is nearer the original estimate (Bhatacharjee and Ferrell, 1983).

Because the viscosity exponent is not established, the predicted values of the decay rates close to the critical temperature are very uncertain. Figure 4 shows the scaled decay rate calculated with two fits to the Strumpf xenon viscosity data (using the exponents 0.065 and 0.054) extrapolated into the temperature range of the space experiment which we are discussing. The difference grows to 10% and illustrates why we must measure the decay rates in this region. They simply cannot be calculated with the limited viscosity data available: even with improvements to viscosity data from a low-gravity experiment, they would still need to be extrapolated into the temperatures reached in this scattering experiment. We do not know whether the equations used for binary mixtures (Burstyn and Sengers, 1982; Kopelman, 1983) will work for a liquid-vapor system. The only way to determine this is to have measurements close to the critical point *without the distortions in the density of the sample induced by gravity*.

We see this experiment as a means to probe the fundamental dynamics of a critical system, specifically that of a simple fluid, by accurately measuring the critical fluctuation decay rates closer to the critical point than is possible in any earth-bound experiment. We expect to measure the actual limiting decay rates at finite wavevector and determine their wavevector dependence. In addition, we will measure the correlation length of the fluctuations. As discussed above, it is not possible at present to calculate the decay rates to the accuracy with which they can be measured in this experiment. Thus, it is a worthy goal to make such a set of measurements on a carefully chosen, simple fluid system like

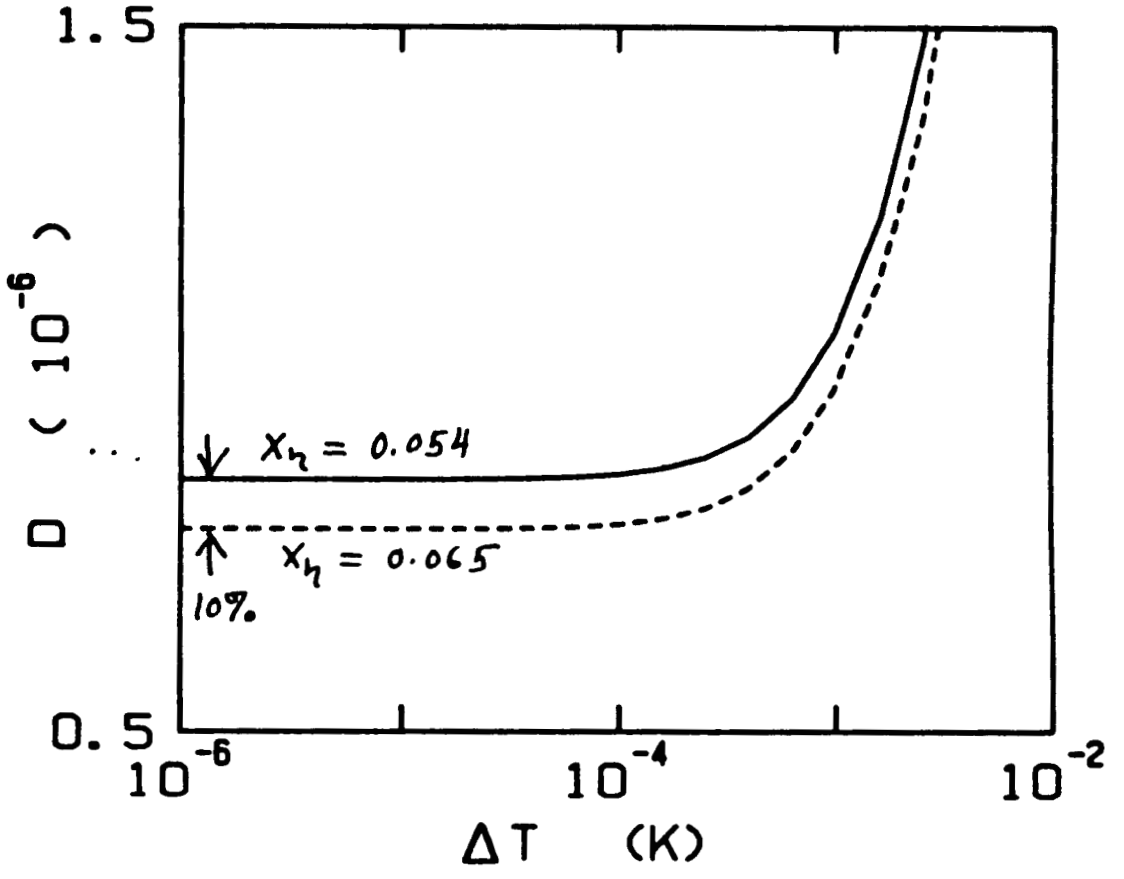

Figure 4. Calculated diffusivity of xenon at a scattering angle of 12°.

xenon. This *data set* will have a lasting value as a testing ground for any ideas about transport properties and dynamics in thermodynamic systems with large fluctuations.

3 Zeno Science Requirements

The list of science requirements distills the experiment into its barest essentials, to provide a foundation on which to build engineering requirements. The list derives from two principle considerations.

First, there are two major measurement goals of the experiment, namely decay rates and correlations lengths of critical fluctuations. Further, the decay rate measurements are to be performed at two angles to fix their dependence on the scattering wavevector. The associated science requirements specify the conditions that must be met to accomplish the precision and range of the measurements that will lead to a satisfactory data set.

1. Determine the decay rates of critical fluctuations in xenon.
    1.1. Measure to $\pm 1\%$ from correlation functions.
    1.2. Measure at two angles, θ and $\pi - \theta$ ($\theta \cong 12°$), with angles known to $\pm 0.03°$.
    1.3. Maintain the multiple scattering below 1% of the scattered intensity.
    1.4. Measure over a temperature range of 1 K to 100 μK from the critical point, with at least two values per decade.
2. Determine the correlation length of critical fluctuations in xenon.
    2.1. Measure to $\pm 3\%$ from transmission and intensity data.
    2.2. Measure time-averaged transmission continuously, to $\pm 0.1\%$.
    2.3. Measure the scattered intensity continuously, to $\pm 0.1\%$.
    2.4. Measure over a temperature range of 1 K to 100 μK from the critical point, with at least two values per decade.
3. Establish the thermodynamic trajectory towards the critical point of xenon.
    3.1. Measure and control the temperature of the sample to ± 3 μK for periods of at least 3 hours.
    3.2. Locate the critical temperature of the sample to ± 20 μK.
    3.3. Establish the absolute temperature of the critical point to ± 10 mK.
    3.4. Load the sample cell to within $\pm 0.1\%$ of the critical density of pure xenon.

3.5. Allow no temperature gradients across the sample larger than 1 μK/cm.

3.6. Limit residual and vibrational accelerations to $\leq 10^{-3}$ g.

3.7. Limit radiation heating of the sample to < 1 μW.

4 The Zeno Experiment

The instrument which performs the experiment divides easily into two subsystems. The optics subsystem includes the xenon sample under study, the means to maintain its thermodynamic state, the light source to probe its fluctuations, and the optical, thermal, and mechanical transducers which monitor its environment and collect the results of the interaction between light and critical fluid. The electronics subsystem oversees the control of the sample's environment, collects information from the transducers, and processes, reports, and stores the information. The operating of the subsystems are coordinated by the control software which manipulates the components of the optics subsystem, supervises the components of the electronics subsystem, and directs the experiment so that it can meet its science goals within the mission timeline.

4.1 Optics

4.1.1 Sample Cell

The xenon sample cell, shown schematically in figure 5, contains the sample at its critical temperature of 289 K and critical pressure of 58 atmospheres, while providing optical access for the light scattering measurements. The primary design constraint, to meet the science requirement of less than 1% multiple scattering, is that the laser beam have a 100 μm path length through the fluid, accomplished simply by having the windows of the sample cell separated by this amount. However, this would create such a small total volume of sample that meeting the science requirement that the cell be loaded to within 0.1% of the critical density would be difficult. Thus, the 100 μm sample space is surrounded by a reservoir of xenon sample, but the reservoir must be designed carefully. If its volume is too large, the heat capacity of the xenon would begin to slow the response of the thermostat. If its surface to volume ratio is too small, the divergent thermal conductivity of xenon at its critical point would lead to unacceptably long thermal relaxation times.

4.1.2 Thermostat

The only parameter controlling the thermodynamic state of the xenon sample is temperature; this is the responsibility of the thermostat. To achieve the goals of the experiment,

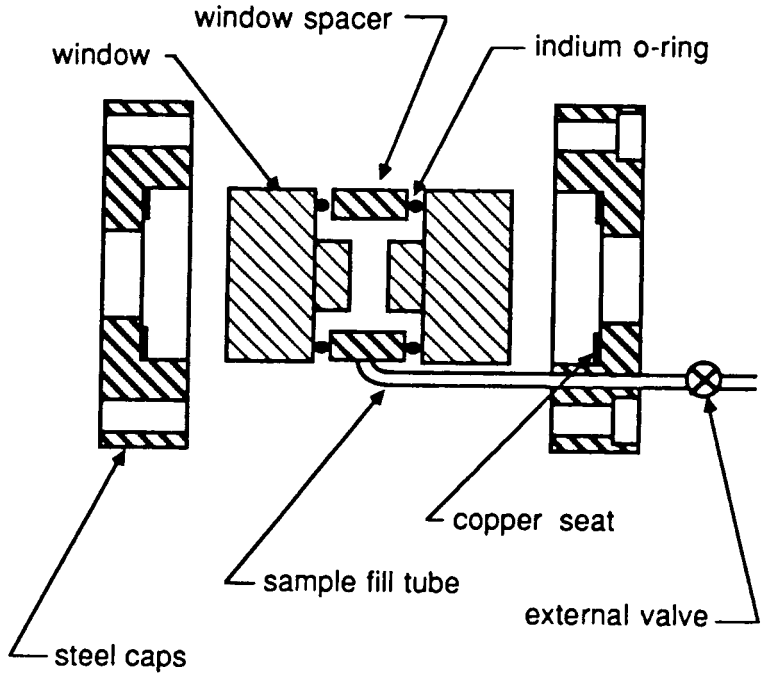

Figure 5. Xenon sample cell with 100 μm optical path length.

the requirements that it must satisfy are severe: controlling and measuring the temperature of the sample to $\pm$ 3 μK (near a temperature of 298 K), and preventing temperature gradients across the sample larger than 1 μK/cm. Furthermore, for its trip into space, the thermostat must be small, lightweight, and able to change temperature quickly to meet accommodation and mission time restrictions.

The thermostat shown schematically in cross section in figure 6 satisfies these goals, assuming an ambient environment stable only to $\pm$ 1 K. It is constructed of four co-axial cylindrical shells (numbered 1 through 4, innermost to outermost), with the sample cell contained within shell 1. The thermal coupling between shells is radiant, with 15 minute time constants. Optical access to the interior is provided by windows mounted on the ends of each shell. The overall size is 16 cm by 7 cm diameter, and the mass is less than 1.5 kg.

Mounted on shell 1 is a platinum resistance thermometer, used for absolute temperature calibrations; in operation, temperature sensing is done with thermistors. Each shell has at least one thermistor mounted on its surface to monitor temperature. On each of the outer three shells, the thermistor is part of a feedback circuit, which includes surface-mounted heaters on the shell, to control the temperature of the shell. Proceeding inward, each shell reduces temperature gradients by a factor of 100.

4.1.3 Optical Paths

A schematic layout of the optical configuration is shown in figure 7. The layout satisfies the science requirements for measuring fluctuation decay rates at two scattering angles and the correlation length of the fluctuations.

The beam from the low-power (5 mW) Helium-Neon laser can take one of two paths through the xenon sample; the path is chosen by the shutters, only one of which is open at a time. In the forward scattering configuration (top of figure 7), part of the beam is deflected into a photodiode to provide a reference for turbidity measurement. The remainder, focused by a lens, passes through the thermostated sample. The light which is scattered by fluctuations in the sample into a small solid angle (defined by the pinholes) at angle θ is collected for decay rate analysis by the photomultiplier tube. That light which survives its trip through the sample unscattered is directed to a second photodiode.

In the backscattering configuration (bottom of figure 7), the beam follows in reverse the path of the forward scattering beam. Again, part of the beam is deflected into a photodiode for turbidity reference. The remainder is focused and passes through the sample. That which makes it through unscattered is collected by another photodiode. The light scattered by the fluctuations in the sample is still collected by the photomultiplier tube, but the scattering angle is now $\pi - \theta$, the supplement of the forward scattering angle.

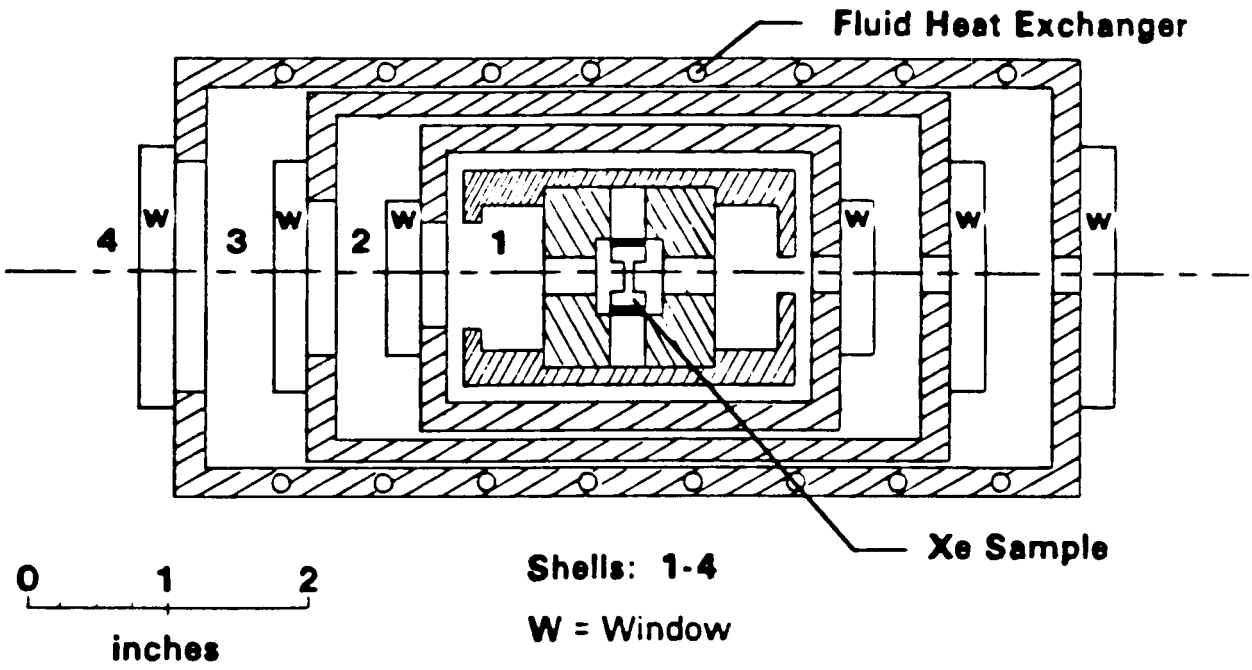

Figure 6. Thermostat

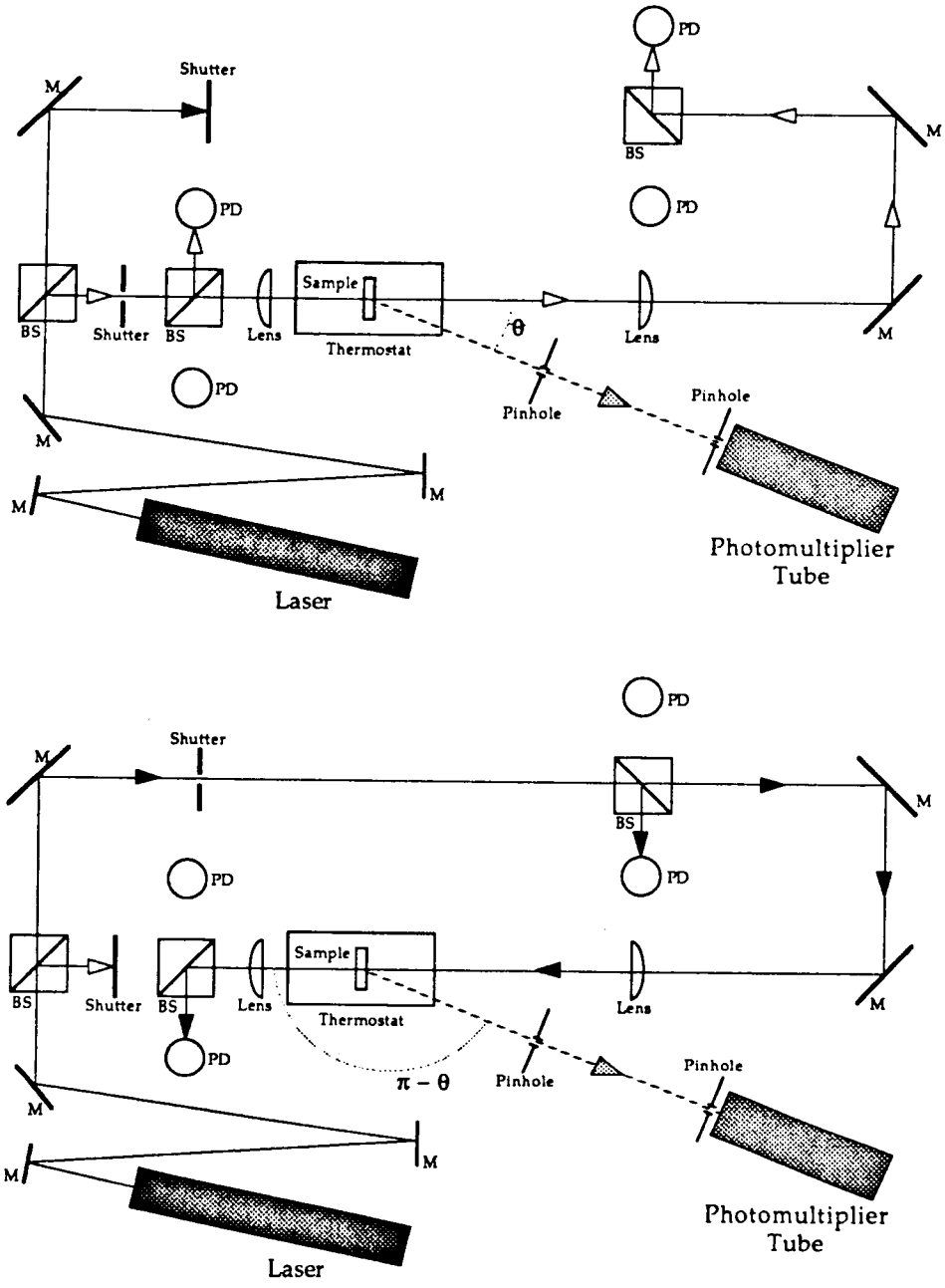

Figure 7. Optical layouts: forward scattering (top) and backscattering (bottom)

4.1.4 Mechanical Environment

The degree to which the experiment achieves its scientific goals increases in proportion to the degree to which it is isolated from vibrations on the STS. Thus the table on which the optics are mounted, beyond providing a stable surface to prevent distortion of the optical paths, is a component of a vibration isolation system to protect the optics subsystem.

Adjunct to the isolation system is the means for real-time monitoring of disturbances passes to the table from the STS. A high dynamic-range triaxial accelerometer is mounted on the surface of the optical table to inform the operating software of vibrational disturbances, also providing information on the size and duration of the disturbance.

4.2 Electronics

The electronics which support the experiment provide five basic functions: thermometry and temperature control, processing of the light scattering signal, processing of the turbidity signal, processing of the accelerometer signal, and opening and closing the shutters which set the scattering configuration. These operations are under the control of a microcomputer which coordinates them and effectively runs the experiment. The system is shown in figure 8.

4.2.1 Temperature Measurement and Control

Thermometry is done using AC bridge circuitry, where one of the bridge is formed by a thermistor and reference resistor (located on each of the thermostat shells), and the other arm is provided by a ratio transformer. The bridge is nulled (i.e. temperature is measured) by changing the tap position in the ratio transformer; null detection is accomplished with a phase sensitive, lock-in amplifier. Using AC signals to excite the bridge with lock-in signal recovery is necessary to achieve the temperature resolution required by the experiment. The output of the lock-in amplifier is a DC voltage representing the amount by which the bridge is out of balance. In the case of the shell 1 thermometer, this error signal represents the temperature of the sample. in the case of the outer shells (2, 3, and 4) the error signal is processed by the temperature controller, which drives heaters mounted on the shells to maintain their temperature, which is set by the ratio transformers. The ratio transformers are in turn set by the microcomputer, in this way determining the temperature profile across the thermostat and monitoring the temperature of the sample via the shell 1 thermometer.

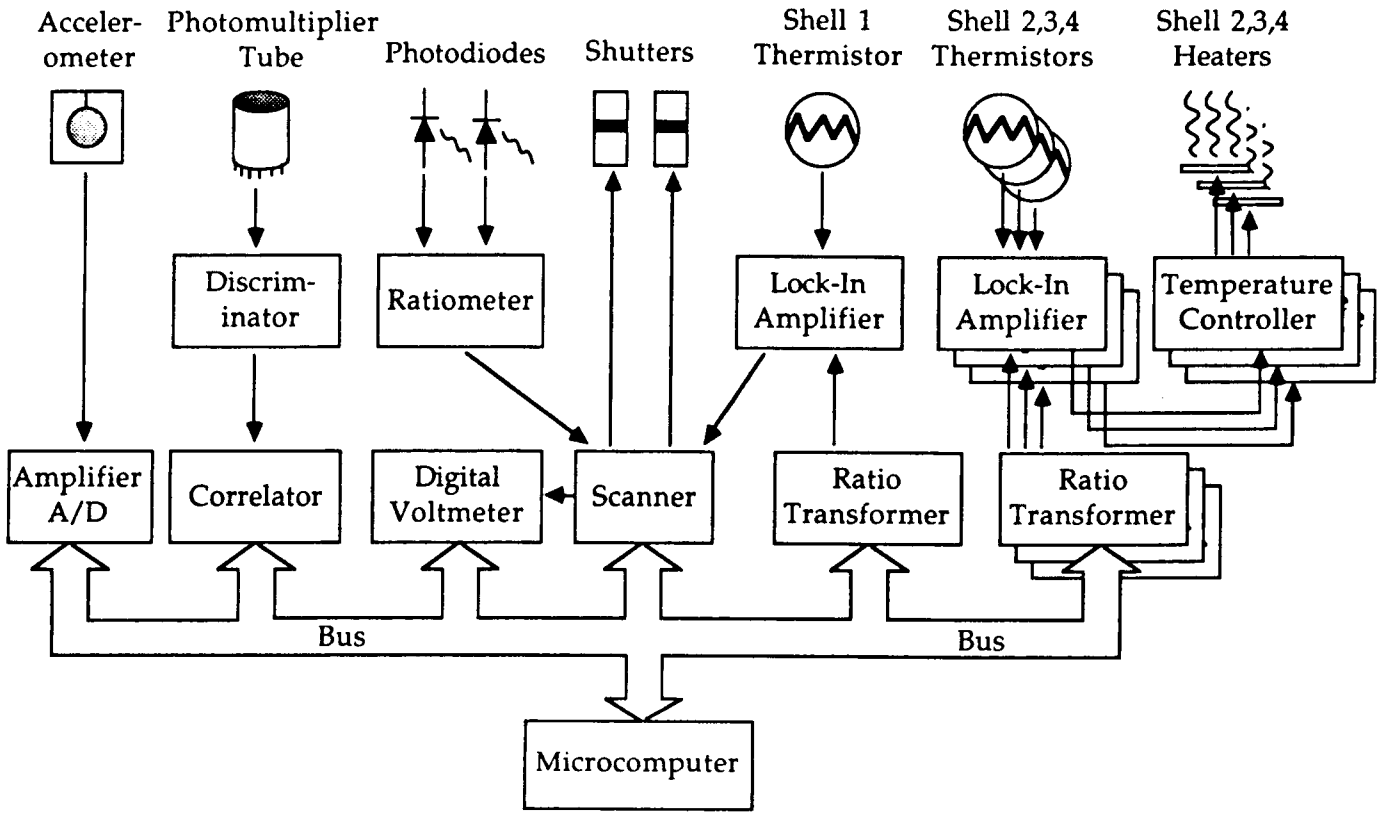

Figure 8. Control and Data Acquisition System

4.2.2 Transducer Signals

The light scattering signal is collected on the optical table by a high-gain, high quantum efficiency photomultiplier tube. The output of the tube is converted by the preamplifier/discriminator into a high-frequency (order MHz) stream of TTL pulses, with the pulse count rate proportional to the intensity of the scattered light. The programmable correlator calculates in real-time the autocorrelation function of the pulse stream as well as the average intensity, then makes the results available to the microcomputer after a pre-determined time. From these data the microcomputer calculates decay rates of the fluctuations, and some of the correlation length information.

In each of the two light path configurations, there is a pair of photodiodes which produce the raw signals for the turbidity measurements. In each case, one photodiode produces a current proportional to the intensity of the test beam to use as an amplitude reference, and a second photodiode produces a current proportional to the intensity of the light transmitted by the sample. The output of the ratiometer circuit is the logarithm of the ratio of transmitted to reference current, which is proportional to the turbidity of the sample. This signal is averaged by a digital voltmeter and passed to the microcomputer.

The signal from the accelerometer mounted on the optical table is processed by its amplifier, and the results passed to the microcomputer when safe levels of acceleration, determined by the current operating temperature of the experiment, are exceeded. With information about the level and duration of the detected disturbances, the control software can choose the proper strategy for accumulating data during the disturbance that takes best advantage of the limited mission time.

4.3 Timeline and Control Software

The software which controls the experiment is responsible for the operation of the electronics, and for coordinating them in the most efficient way to accomplish the science goals. Figure 9 shows a hierarchy of functions to be performed by the control software. Coordination of experimental activity is the primary responsibility of the experiment scheduling program, which decides the optimal approach to data taking, subject to programmmed information from the planned mission schedule and real-time information from the accelerometers located on the optics table. This schedule is passed to the synchronous device controller which is responsible for overseeing the actual operation of the electronics, as well as handling data storage. Some results of the lower lever operations are made known to the scheduling program to inform it of progress. With this feedback the scheduler is able to report both its decisions and the progress of the experiment based on those decisions to a ground-based monitor which can override its decision process.

The time line for the experiment breaks down into four parts:

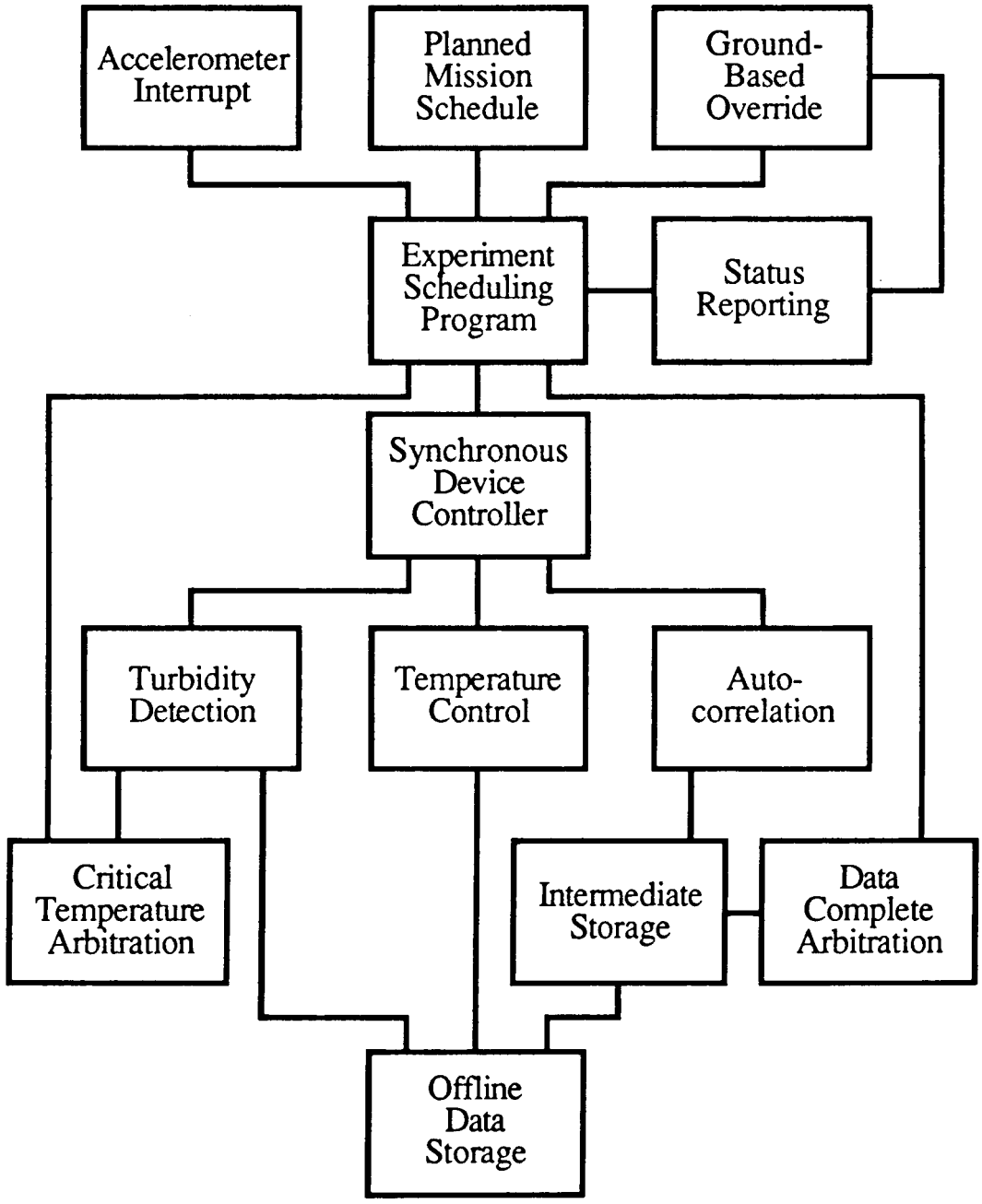

Figure 9. Experiment Control Hierarchy

1. Turn-on, initialize, and establish stating conditions.

2. Locate the critical temperature of the sample.

3. Measure decay rates and turbidity at temperature sequence.

4. Verify the critical temperature of the sample.

The turn-on of the instrument proceeds automatically after being actuated by the STS crew. The xenon sample must be put at a known, equilibrium state at a determined temperature, in order that it be homogeneously mixed and ready for operations. Given intershell time constants in the thermostat of 15 minutes, and an overall time constant of 45 minutes, reaching the initial temperature would take several hours. To allow the sample to equilibrate thoroughly, we allow 6 hours for the initialization procedure.

Locating the critical temperature of the sample is done by first cooling the sample quickly to a temperature near the critical temperature (typically within 100 μK); distance from the critical temperature can be inferred from the turbidity of the xenon sample. Once near the critical point, the thermostat alternately cools and warms the sample, looking for hysterisis in the turbidity signal which marks the beginning of the irreversible spinodal decomposition of the fluid which marks the critical point. The final steps in the cooling and warming are made at the temperature resolution of the thermostat, establishing the critical temperature of the sample to 100 μK. At present, the most length searches performed in the laboratory take from 4 to 6 hours; for the mission, we allow 8 hours as an upper bound and expect the actual time needed to be shorter.

The turbidity and fluctuation decay rates of the xenon sample are to be measured throughout the temperature range of 1 K to 100 μK from its critical point. Depending on the severity of the vibration environment encountered by the experiment, this range could be extended from 1 K to 3 μK. We plan to take measurements at a sequence of temperatures of two per decade, at temperature differences of 1 K, 0.3 K, 0.1 K,..., 3×10^{-5}K, 10^{-6}K, 3×10^{-6}K. The last points will be more difficult than the first and may require extra attention. Thus, the sequence will have about 12 temperature points as a minimum set. At each temperature a sequence of forward ($\theta = 12°$) and backward ($\theta = 168°$) scattering fluctuation decay rates will be taken automatically by the correlator and analyzed, alternating between forward and backscattering configurations. Fitted correlation functions give the experimentally determined decay rate. These are compared as they accumulate; when the prescribed statistical accuracy is achieved, that determination is considered complete and the microcomputer moves the experiment on to the remaining temperatures.

Each correlation takes about 15 minutes for reasonable statistics and 10 points at each angle should reduce the statistical uncertainty of the decay rates to the required accuracy

6 References

Beysens, D. and G. Zalczer (1977), Phys. Rev. **A15**, 765.

Bhattacharjee, J. K., R. A. Ferrell, R. S. Basu, and J. V. Sengers (1981), Phys. Rev. **A24**, 1469.

Bhattacharjee, J. K., and R. A. Ferrell (1983), Phys. Rev. **A28**, 2363.

Bray, A. J. and R. F. Chang (1975), Phys. Rev. **A12**, 2594.

Burstyn, H. C., J. V. Sengers, J. K. Bhattacharjee, and R. A. Ferrell (1983), Phys. Rev. **A28**, 1567.

Burstyn, H. C. and J. V. Sengers (1982), Phys. Rev. **A25**, 448.

Chang, R. F., H. Burstyn and J. V. Sengers (1979), Phys. Rev. **A19**, 866.

Cohen, L. H., M. L. Dingus and H. Meyer (1982), J. Low Temp. Phys. **A49**, 545.

Cohen, L. H., M. L. Dingus and H. Meyer (1983), Phys. Rev. Lett. **50**, 1058.

Güttinger, H. and D. S. Cannell (1980), Phys. Rev. **A22**, 285.

Kawasaki, K. (1976), in *Phase Transitions and Critical Phenomena* ed. C. Domb and M. S. Green (Academic, New York, 1976), Vol. 5A, p. 165.

Kopelman, R. B. (1983), Ph. D. thesis, University of Maryland, "Light Scattering Measurements of Critical Fluctuations in an Optically Thin Binary Liquid Sample".

Reith, L. A. and H. L. Swinney (1975), Phys. Rev. **A12**, 1094.

Sengers, J. V. (1982), from *Phase Transitions: Cargese 1980*, ed. Maurice Levy, Jean-Claude Le Guillou, and Jean Zinn-Justin (New York: Plenum Publishing Corporation).

Siggia, E. D., B. I. Halperin and P. C. Hohenberg (1976), Phys. Rev. **B13**, 2110.

Sorenson, C. M., R. C. Mockler and W. J. O'Sullivan (1977), Phys. Rev. **A16**, 365.

Swinney, H. L. and D. L. Henry (1973), Phys. Rev. **A8**, 2586.

of 1%. The switch between forward and backscattering configurations is accomplished by the shutters on the optical table in less than 1 second. During the time that correlation functions are accumulating (in either configuration), the turbidity of the sample is logged continuously at the rate of approximately 1 sample/second. Thus the time for accumulating the correlation functions sets the time scale of the experiment at 6 hours per temperature point or a total of 78 hours.

If more time is available to the experiment during this phase, then the control program would concentrate on obtaining additional information in the temperature range from 3 mK to 3 μK from the critical point, the range in which earthbound measurements are impossible. Note that, for the self-consistency and integrity of the data set for post-flight analysis, we do take time to measure the turbidity and decay rates rather far from the critical temperature.

Finally, to check for possible (but unexpected) drifts in the thermometry, the experiment will verify its earlier determination of the critical temperature. We expect again that this will take no longer than 8 hours.

Thus, the total time line is made up of 6 hours to establish initial operating conditions, 8 hours for locating the critical temperature of the xenon sample, 78 hours for completing the turbidity and decay rate data set, and a final 6 hours for verifying the critical temperature, for a total mission time of 100 hours. We expect that some of the start-up time and time for locating the critical temperature can be eliminated. If more time is available for data taking, the measurements can be made in a smaller temperature sequence concentrating on the smaller temperature differences.

5 Acknowledgements

This project is currently funded under NASA grant NAG3-727 through NASA/Lewis Research Center. The Lewis project manager is Dr. R. Lauver. The project has been named Zeno after the Greek philosopher famous for his paradoxes about limits.

The principal investigator wishes to acknowledge his many collaborators in this project. The principal scientist for the project is Dr. J. Shaumeyer, who has made major contributions to all phases of the work and particularly to the automation of the present laboratory prototype of the experiment. University of Maryland graduate students M. Briggs and H. Boukari have each taken on portions of the lab work. Many of the design ideas have been developed and refined with the help of our design subcontractor Ball Aerospace Systems Division, with the team under project manager Dr. R. Reinker.